Supporting information

Conformation Sensitive Targeting of Lipid Nanoparticles for RNA Therapeutics

Niels Dammes[1-4], Meir Goldsmith[1-4], Srinivas Ramishetti[1-4], Jason L. J. Dearling[5], Nuphar Veiga[1-4], Alan B. Packard[5] and Dan Peer[1-4]

[1.]Laboratory of Precision Nanomedicine, Shmunis School of Biomedicine and Cancer Research, George S. Wise Faculty of Life Sciences, [2.]Department of Materials Sciences and Engineering, Iby and Aladar Fleischman Faculty of Engineering, [3.] Center for Nanoscience and Nanotechnology; [4.]Cancer Biology Research Center, Tel Aviv University, Tel Aviv, 69978, Israel.[5.] Division of Nuclear Medicine and Molecular Imaging, Department of Radiology, Boston Children's Hospital, Boston, MA; †Harvard Medical School, Boston, MA 02115, USA

[*]**Correspondence: Dan Peer, e-mail: peer@tauex.tau.ac.il**

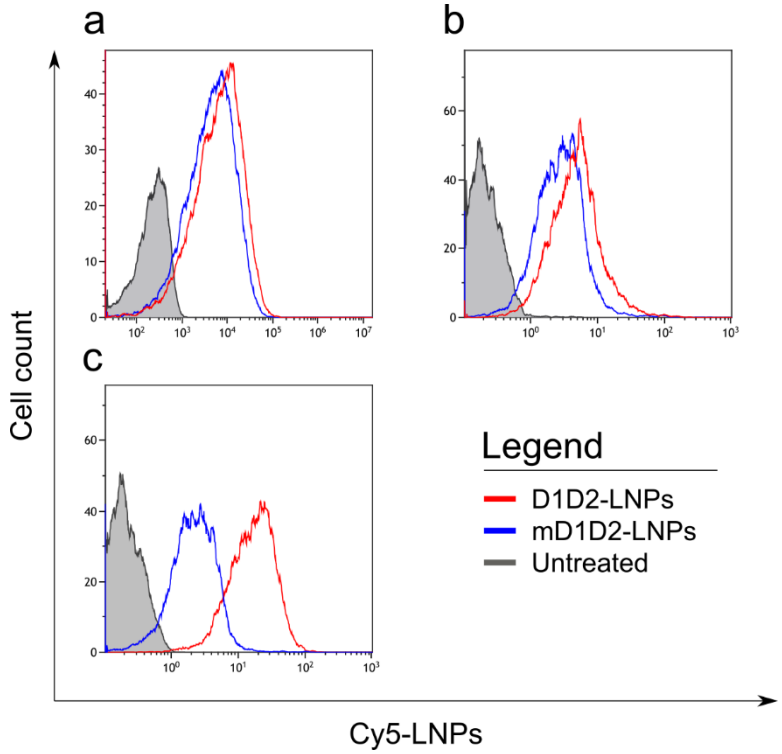

Supplementary Figure 1 | Comparison of LNP functionality between different conjugation methods. **(a)** Direct conjugation of the D1D2 protein by reducing the cysteine residues in the D1D2 protein followed by covalent attachment to the maleimide groups on the DSPE-PEG lipid on the LNP. **(b)** Conjugation by using the ASSET linker (lipidated scFv against rat IgG_{2a}-Fc) which in turn binds the D1D2 protein by affinity to the Fc domain. **(c)** Chemical conjugation of the RG7 monoclonal antibody (mouse anti rat IgG_{2a}) which in turn binds the D1D2 protein by affinity to the Fc domain. The last method is far superior to the other two methods with regard to LNP binding to TK-1 cells *in vitro*.

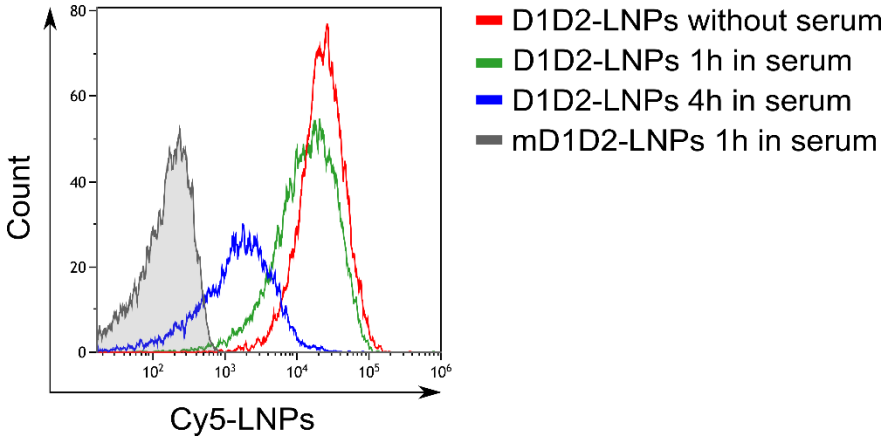

Supplementary Figure 2 | *In vitro* incubation of D1D2-conjugated LNPs (through the RG7 linker) in mouse blood plasma at 37°C followed by testing the LNP binding capability to TK-1 cells. Although 4 h incubation in plasma reduced the binding to TK-1 cells, the difference between mD1D2 and D1D2 after 1 h in serum is substantial. This should provide enough time for the LNPs to bind to leukocytes *in vivo*.

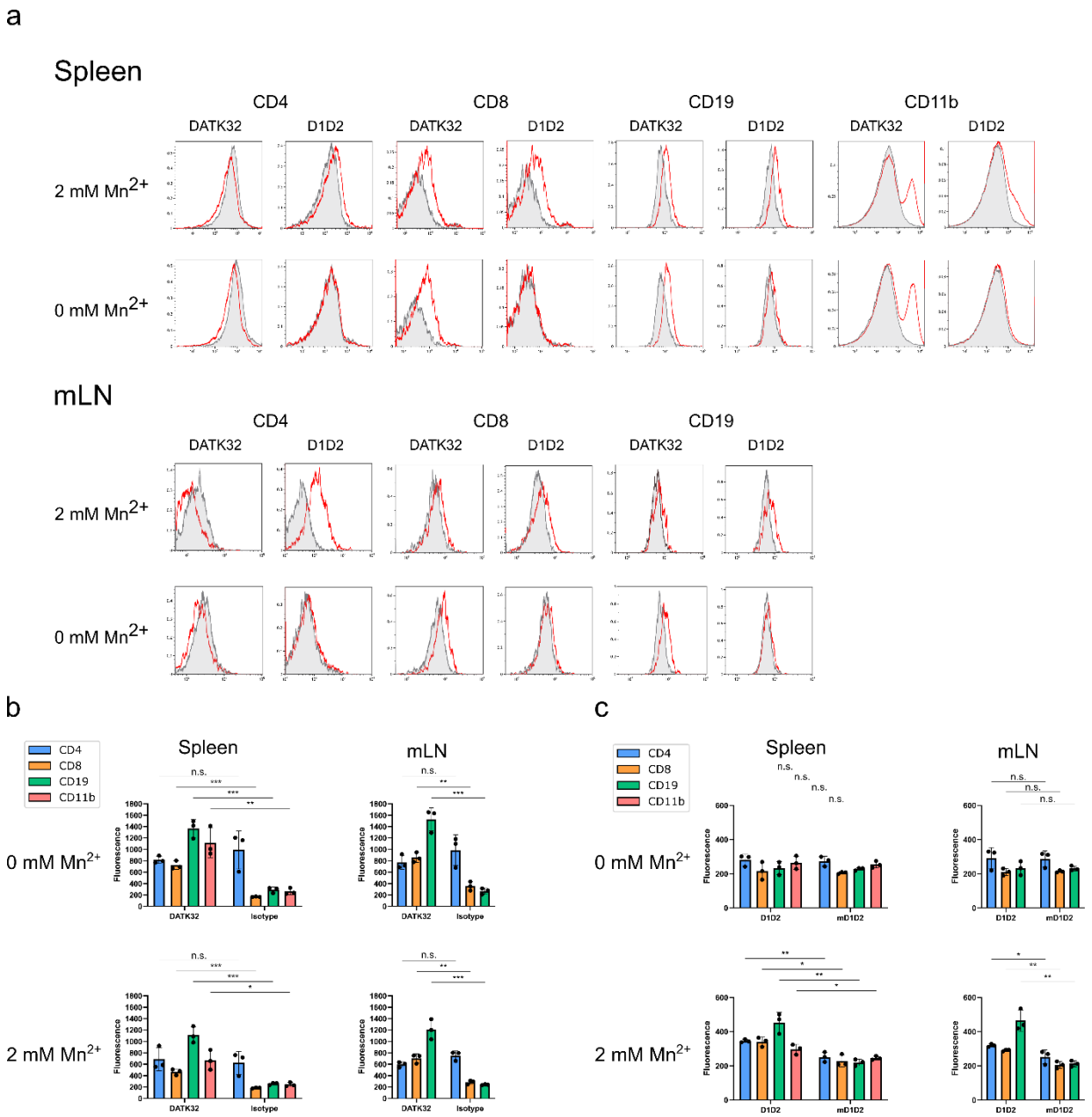

Supplementary Figure 3 | Ex vivo binding of either D1D2-targeted LNPs or DATK32-targeted LNPs to leukocytes from the spleen and mesenteric lymph nodes (mLN) of mice with colitis. (a) Binding was analyzed by flow cytometry and compared to the negative control: isotype control (for DATK32) or the mD1D2 (for D1D2), which is displayed in grey. Binding to Mn^{2+}-treated cells was compared to cells without Mn^{2+} treatment to verify conformational specificity. As expected, the DATK32 antibody was unable to distinguish between HA and LA $\alpha_4\beta_7$ integrin (as it displays similar binding levels between the Mn^{2+}-treated group and the control group). D1D2, on the other hand demonstrated a strong binding preference to Mn^{2+}-activated cells. Surprisingly, the DATK32 mAb was, when conjugated to the LNPs, unable to bind to CD4+ T-cells. **(b)** Quantification of *ex vivo* binding results for DATK32. **(c)** Quantification of *ex vivo* binding results for D1D2. Data shows mean fluorescence intensity +/- SD. Statistical significance was calculated using a two-sided t-test for each subpopulation, n = 3 mice, * $p < 0.05$, ** $p < 0.01$, *** $p < 0.001$, n.s. = not significant.

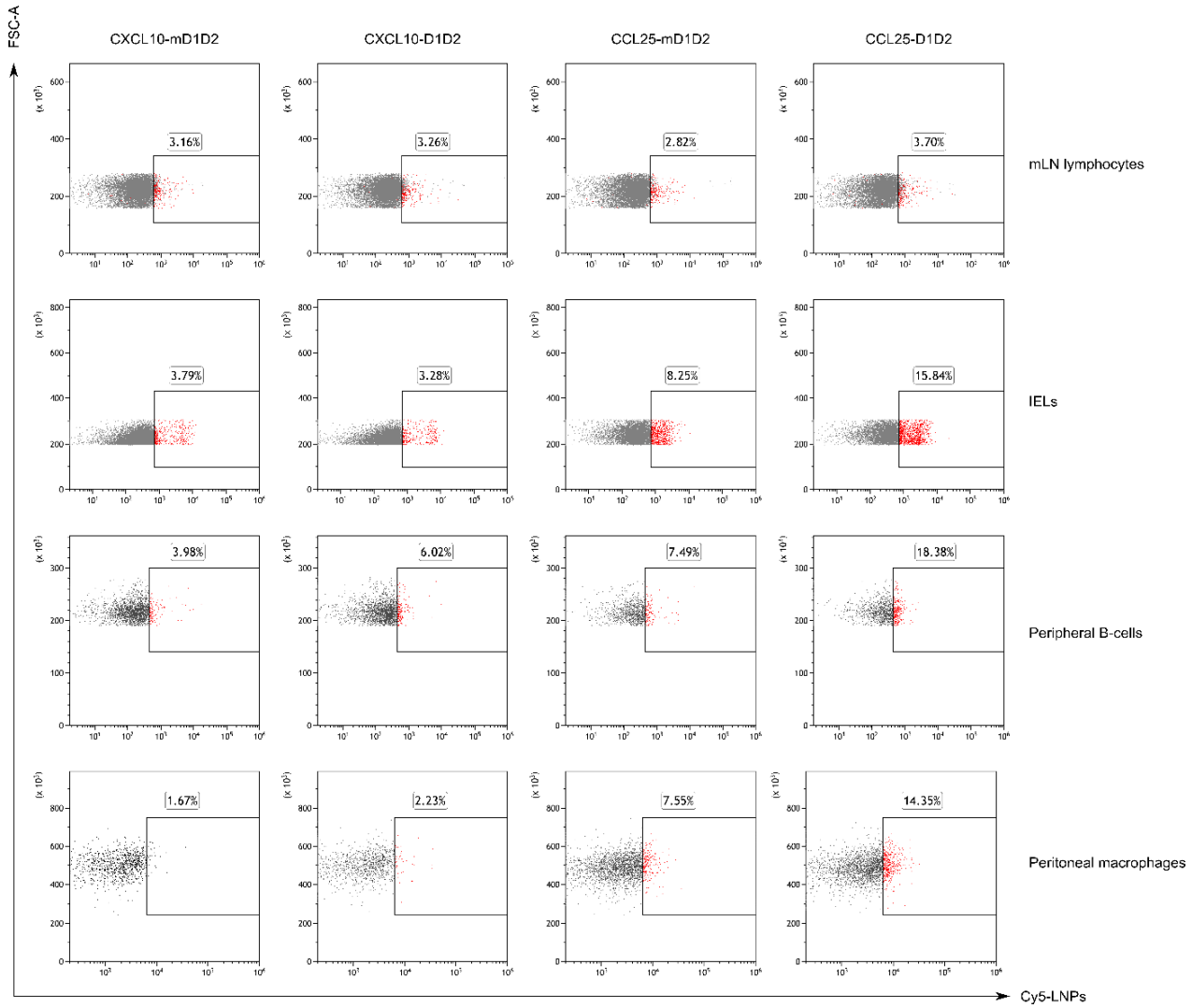

Supplementary Figure 4 | Chemokine activation using CCL25 specifically increases LNP binding to primary leukocytes when compared to CXCL10-treated control cells.

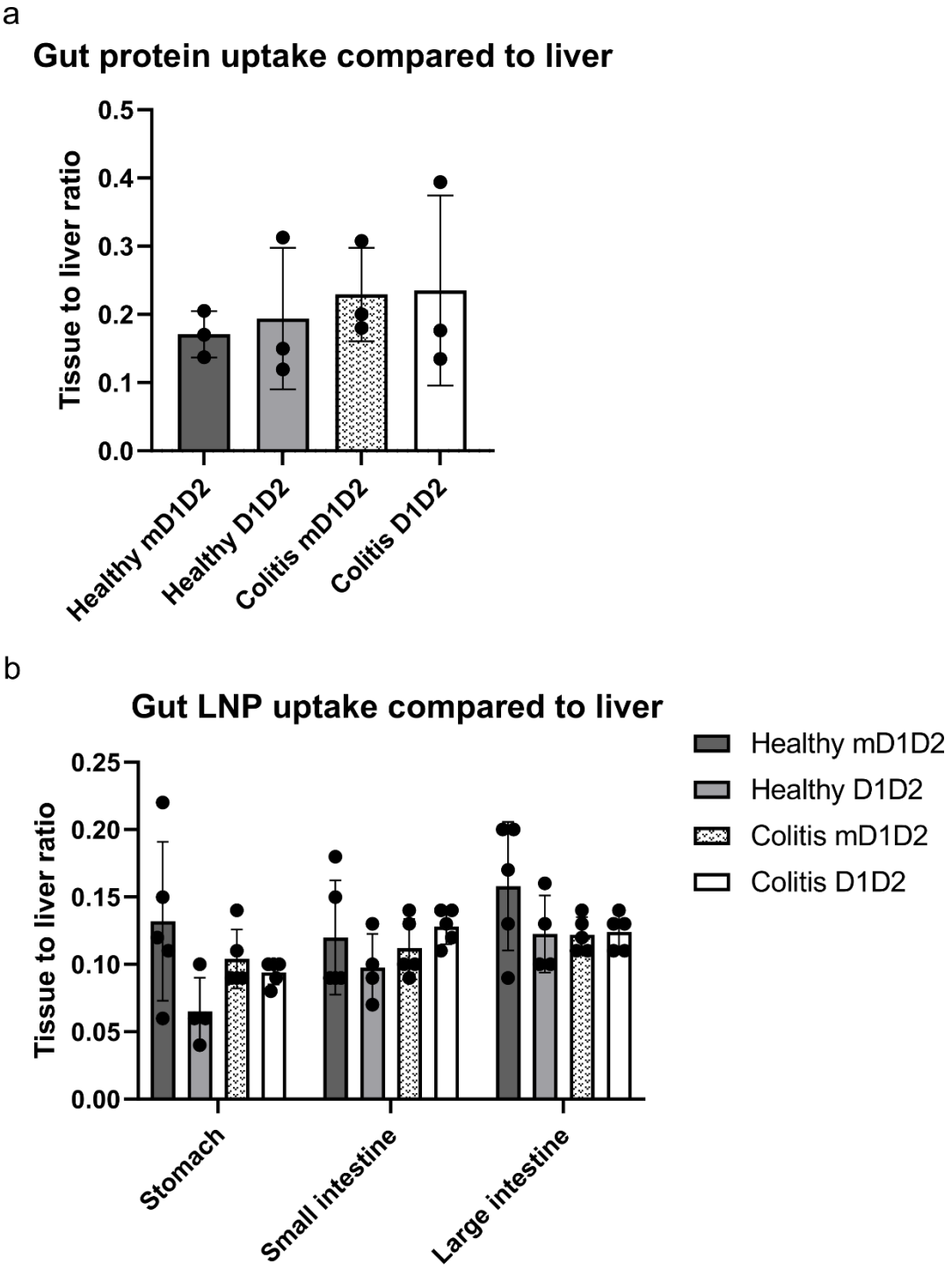

Supplementary Figure 5 | Gut uptake as a ratio of liver uptake of both the free D1D2 protein and the targeted LNPs. (a) Uptake of radiolabeled protein, n = 3 mice. **(b)** Uptake of radiolabeled LNPs, n = 5 mice. No significant differences in gut:liver ratios were observed, probably due to the high signal in the liver. Data in both **(a)** and **(b)** are represented as mean values +/- SD.

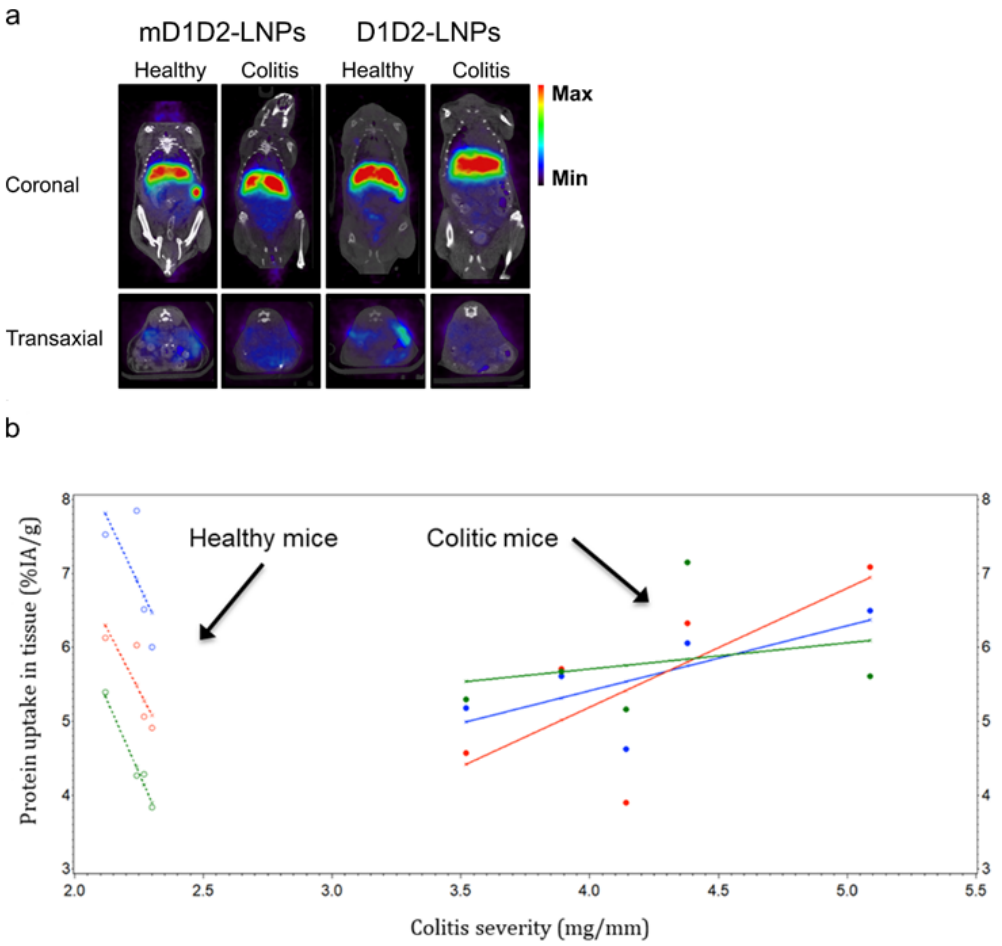

Supplementary Figure 6 | Radiolabeled LNP uptake and uptake of radiolabeled D1D2 protein increases with degree of colitic disease in a piroxicam-induced mouse model of colitis. (a) Representative microPET/CT images showing distribution of LNPs in healthy mice and mice with active colitis. **(b)** Protein uptake is plotted against colonic density (degree of colitis) for each of the 3 tissue types of major interest (**large intestine**, **small intestine**, **stomach**). For the animals with colitis, uptake of the target-binding protein increased with colitis severity (solid lines to right of the graph), while for the control animals, protein uptake decreased (dashed lines to left). The slopes (se) for the large intestine, small intestine, and stomach were positive for colitis mice (0.88 (0.57), 1.61 (0.71), and 0.36 (0.59)), and negative for control mice (-7.39 (4.94), -6.60 (6.12), and -8.32 (5.07)).
The (colitis – control) differences (se) of these slopes were similar across the three tissues: 8.27 (4.98), 8.20 (6.16), and 8.68 (5.11) for the large intestine, small intestine, and stomach, respectively. The similarity of (colitis – control) differences of slopes was confirmed by fitting a 2-way interaction mixed model (containing fixed and random effects) using the data for all tissue types. The common estimate (se) based on this model was 8.38 (3.41). The p-value corresponding to the null hypothesis of equal colitis and control slopes was $p = 0.014$, indicating >95% confidence that there is a difference between the slopes of the two populations.

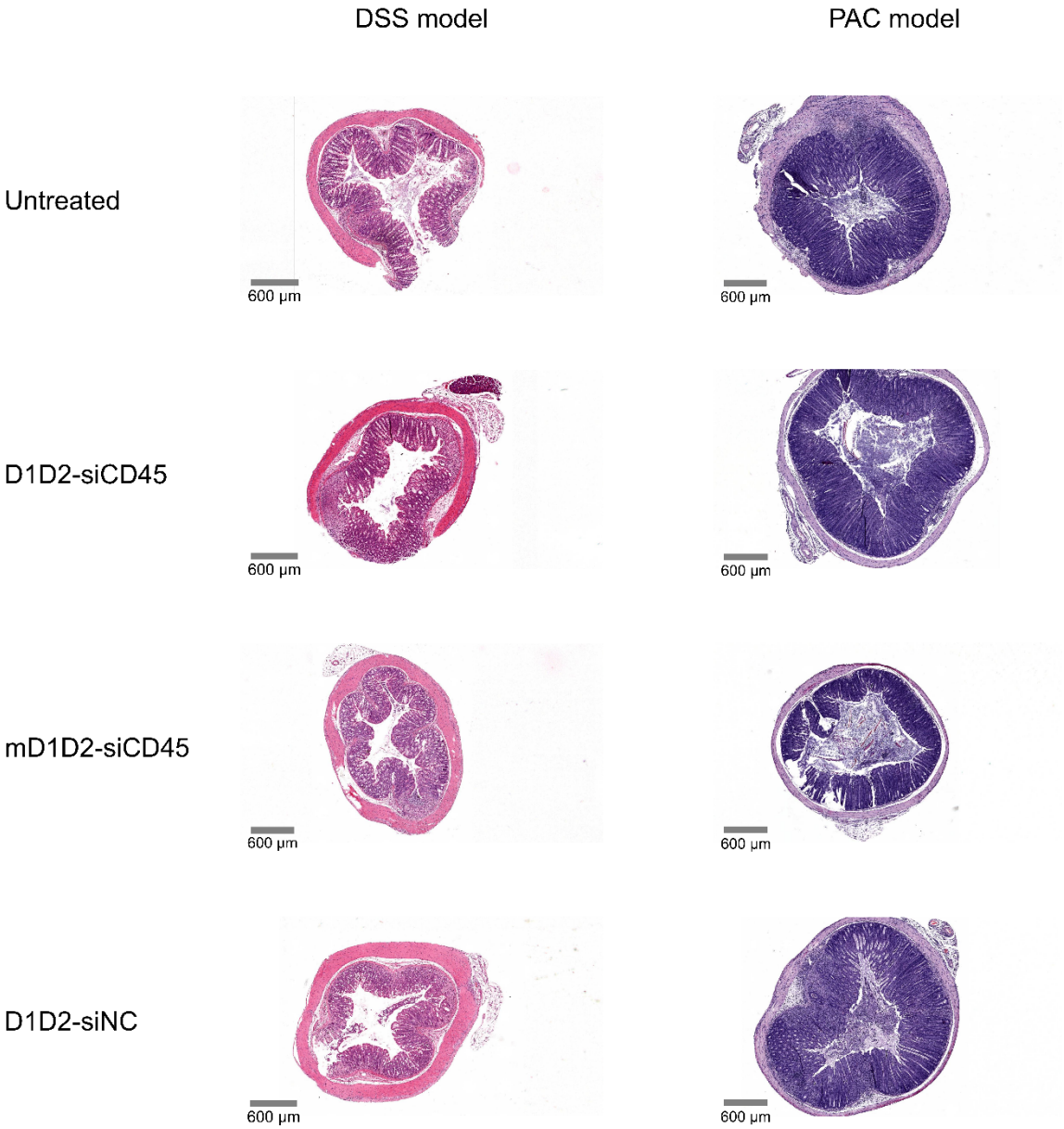

Supplementary Figure 7 | Colon histology of mice with either PAC or DSS-induced colitis. A comparison between the different LNP formulations of the CD45 silencing experiment shows that the LNPs do not alter the colon visibly. Reported differences are only made between groups using the same model.

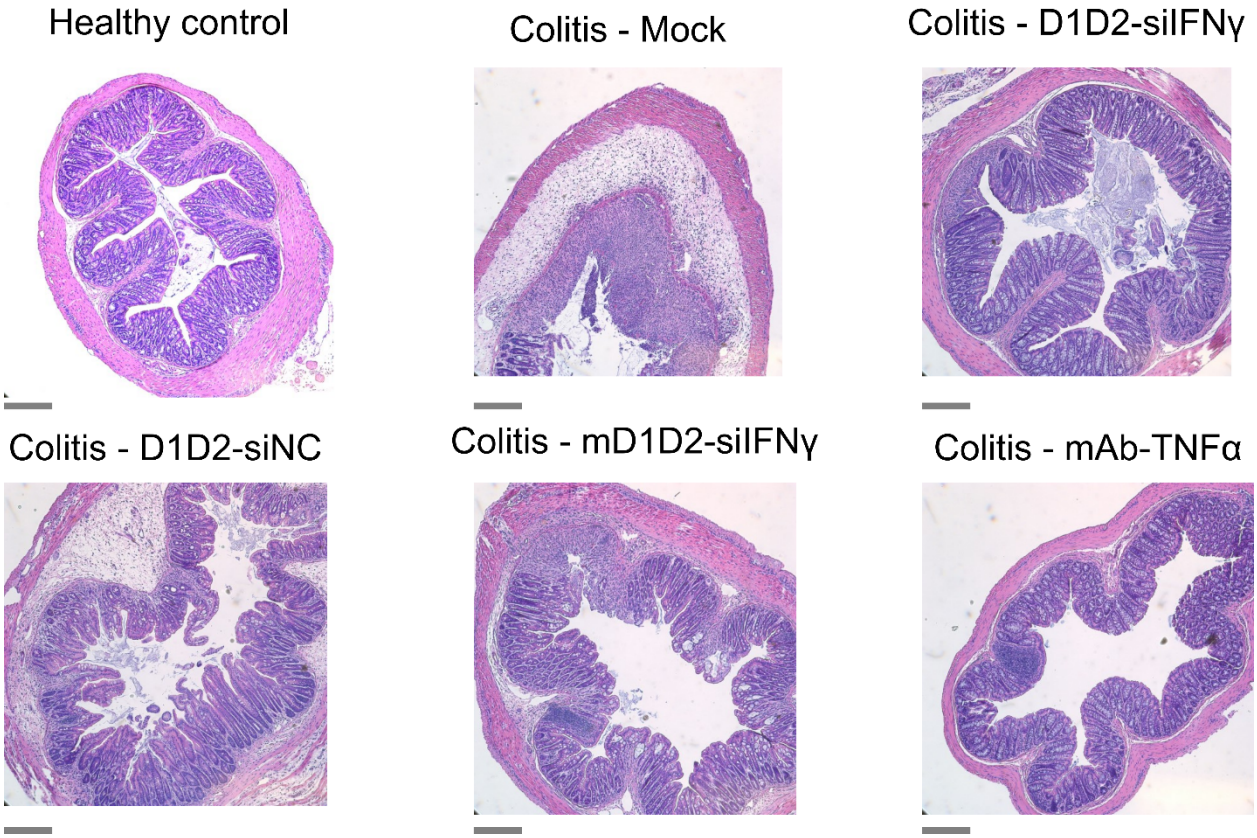

Supplementary Figure 8 | Representative photomicrographs of colon cross sections for each group of the therapeutic efficacy experiment using siRNA against IFNγ. Experiment was repeated 3 times independently. Grey scale bar represents 750 μm.

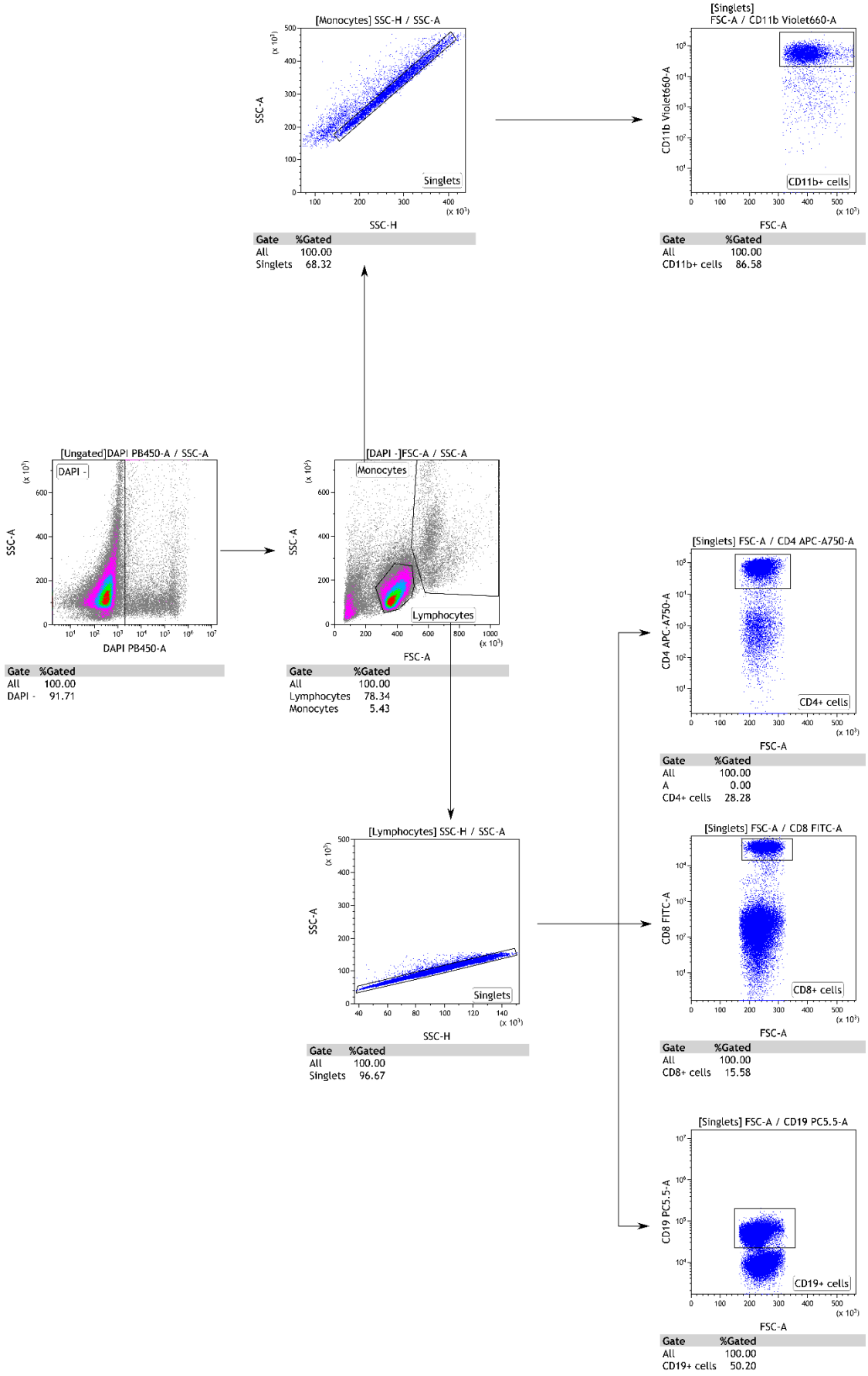

Supplementary Figure 9 | Gating strategy for flow cytometry experiments using cells from the spleen. Input gate for each graph is indicated above the graph in square brackets.

DNA Sequence

ATGGAGACTGGGCTGCGCTGGCTTCTCCTGGTCGCTGTGCTCAAAGGTGTCCAGTGTGACTACAAAGACGATGACG
ACAAGCTTGCGGCCGCGCAGTCCTTCCAGGTGAACCCCCCTGAGTCTGAGGTAGCTGTGGCCATGGGCACATCCCTC
CAGATCACCTGCAGCATGTCCTGTGACGAGGGTGTAGCCCGGGTGCACTGGCGTGGTCTGG**A**CACCAGCTTGGGCA
GTGTACAGACCCTCCCAGGCAGCAGTATCCTCTCTGTACGGGGCATGCTGTCAGACACAGGCACTCCTGTGTGTGTG
GGCTCCTGCGGGAGTCGAAGCTTCCAGCACTCCGTGAAGATCCTTGTGTATGCCTTCCCAGACCAGCTGGTGGTGTC
CCCGGAGTTCCTTGTACCTGGACAGGACCAGGTGGTGTCCTGCACGGCCCACAACATCTGGCCTGCAGACCCGAAC
AGTCTCTCCTTTGCCCTGCTACTGGGAGAGCAGAGACTGGAGGGTGCCCAAGCCCTGGAACCAGAGCAAGAAGAG
GAGATACAAGAGGCTGAGGGCACACCACTGTTCCGAATGACACAACGCTGGCGGTTACCCTCCCTGGGGACCCCTG
CCCCTCCTGCCCTTCACTGCCAGGTCACCATGCAGCTGCCCAAACTGGTGCTGACCCATAGAAAGGAGATTCCAGTG
CTGGGCGGAGGCGGGAGCGGAGGCGGAGGGTCCGGAGGCGGCGGGAGCGTGCCAAGGGAATGCAATCCTTGTG
GATGTACAGGCTCAGAAGTGTCATCTGTCTTCATCTTCCCCCCAAAGACCAAAGATGTGCTCACCATCACTCTGACTC
CTAAGGTCACGTGTGTTGTGGTAGACATTAGCCAGAATGATCCCGAGGTCCGGTTCAGCTGGTTTATAGATGACGTG
GAAGTCCACACAGCTCAGACTCATGCCCCGGAGAAGCAGTCCAACAGCACTTTACGCTCAGTCAGTGAACTCCCCAT
CGTGCACCGGGACTGGCTCAATGGCAAGACGTTCAAATGCAAAGTCAACAGTGGAGCATTCCCTGCCCCCATCGAG
AAAAGCATCTCCAAACCCGAAGGCACACCACGAGGTCCACAGGTATACACCATGGCGCCTCCCAAGGAAGAGATGA
CCCAGAGTCAAGTCAGTATCACCTGCATGGTAAAAGGCTTCTATCCCCCAGACATTTATACGGAGTGGAAGATGAAC
GGGCAGCCACAGGAAAACTACAAGAACACTCCACCTACGATGGACACAGATGGGAGTTACTTCCTCTACAGCAAGC
TCAATGTAAAGAAAGAAACATGGCAGCAGGGAAACACTTTCACGTGTTCTGTGCTGCATGAGGGCCTGCACAACCA
CCATACTGAGAAGAGTCTCTCCCACTCTCCTGGTAAAGGCTCCGGCCATCATCACCACCACCATTGA

Amino Acid Sequence

METGLRWLLLVAVLKGVQCDYKDDDDKLAAAQSFQVNPPESEVAVAMGTSLQITCSMSCDEGVARVHWRGL**D**TSLGS
VQTLPGSSILSVRGMLSDTGTPVCVGSCGSRSFQHSVKILVYAFPDQLVVSPEFLVPGQDQVVSCTAHNIWPADPNSLSF
ALLLGEQRLEGAQALEPEQEEEIQEAEGTPLFRMTQRWRLPSLGTPAPPALHCQVTMQLPKLVLTHRKEIPVLGGGGSGG
GGSGGGGSVPRECNPCGCTGSEVSSVFIFPPKTKDVLTITLTPKVTCVVVDISQNDPEVRFSWFIDDVEVHTAQTHAPEKQ
SNSTLRSVSELPIVHRDWLNGKTFKCKVNSGAFPAPIEKSISKPEGTPRGPQVYTMAPPKEEMTQSQVSITCMVKGFYPP
DIYTEWKMNGQPQENYKNTPPTMDTDGSYFLYSKLNVKKETWQQGNTFTCSVLHEGLHNHHTEKSLSHSPGKGSGHH
HHHH

Primer	Function	Sequence (5' → 3')
F1	Amplifies Rat IgG_{2a}-Fc	GAAAACCTGTACTTTCAGGGCGCTGAAACAACAGCCCCATCTGTC
R1	Amplifies Rat IgG_{2a}-Fc	CCTCTAGAGTCGACTGGTACCGATATCAGATCTATCGATGTCATTT ACCAGGAGAGTGGGAGAG
F2	Cloning into pcDNA3.4	CTGGTCGCTGTGCTCAAAGGTGTCCAGTGTGACTACAAAGACGAT GACGAC
R2	Cloning into pcDNA3.4	GATCGAACCCTTGTCGAGGTCGGGGGATCCTCATTTACCAGGAGA GTGGG
F3	Site-directed mutagenesis	GTGCACTGGCGTGGTCTGGCCACCAGCTTGGGCAGTGTAC
R3	Site-directed mutagenesis	GTACACTGCCCAAGCTGGTGGCCAGACCACGCCAGTGCAC
F4	Removes C_H1 domain	GAAAACCTGTACTTTCAGGGCGGTTCTGGTGTGCCAAGGGAATGCA ATCCTTGTGGATGT
R4	Removes C_H1 domain	ACCAGAACCACCTAGTACTGGAATCTCCTTTCTATGGGTCAGCACCA G

Supplementary Figure 10 | DNA and amino acid sequence of the MAdCAM-D1D2-Fc construct and the primers used to clone this. The MAdCAM domains D1 and D2 are underlined. The amino acid that was changed for the mutated control is indicated in bold.